RADIO SCIENCE, VOL. 37, NO. 4, 1053, 10.1029/2000RS002377, 2002

Surface integral equations for material layers modeled with tensor boundary conditions

Erdem Topsakal and John L. Volakis

Radiation Laboratory, Department of Electrical Engineering and Computer Science, University of Michigan, Ann Arbor, Michigan, USA

Daniel C. Ross

Sikorsky Aircraft Corporation, Stratford, Connecticut, USA

Received 27 April 2000; accepted 5 February 2002; published 18 July 2002.

[1] A new class of tensor boundary conditions is introduced for modeling multilayered dielectric structures. Surface integral equations are then developed on the basis of these tensor conditions for a more efficient modeling of nonmetallic bulk structures. Numerical examples are presented to demonstrate the accuracy and applicability of these boundary conditions. *INDEX TERMS:* 0619 Electromagnetics: Electromagnetic theory; 0644 Electromagnetics: Numerical methods; *KEYWORDS:* boundary condition, integral equation, multilayer material, method of moments

1. Introduction

[2] There is significant interest in scattering from thin layers of materials with combined dielectric and magnetic properties [*Harrington and Mautz*, 1975; *Mitzner*, 1968; *Ricoy and Volakis*, 1990; *Puska et al.*, 1999]. The reflection and transmission properties of such systems are relevant in the context of electromagnetic signal processing, frequency-selective surfaces, and radome and antenna design. Numerical simulation of the scattered or radiated fields in the presence of these thin layers becomes significantly less intensive if the layers are modeled using equivalent sheet boundary conditions. In this case, the computational problem is reduced to solving a system of surface integral equations, rather than dealing with volume dielectrics.

[3] In this paper, we propose a new matrix or tensor boundary condition (TBC) for modeling highly inhomogeneous multilayered screens without the need to sample within the volume of such materials. These boundary conditions also have the desirable property of reducing to the usual metallic, resistive, conductive, and impedance boundary conditions. Surface integral equations are subsequently formulated in the context of these tensor boundary conditions. Presented numerical results show the utility and efficiency of the proposed tensor boundary conditions.

0048-6604/02/2000RS002377

2. Formulation

[4] Consider a thin (penetrable or impenetrable) multilayered sheet (see Figure 1a). Our goal is to find an equivalent model (Figure 1b) that is simpler to analyze in the context of integral equation formulations. To do so, we will follow the standard approach [*Senior and Volakis*, 1995] and introduce a mathematical surface or sheet whose reflection properties are the same as those of the original multilayer structure. In this context we propose the dual conditions

$$\begin{aligned}\hat{\mathbf{n}} \times [\mathbf{E}^+(\mathbf{r}) + \mathbf{E}^-(\mathbf{r})] = \hat{R}_e \hat{\mathbf{n}} &\times [\hat{\mathbf{n}} \times \mathbf{H}^+(\mathbf{r}) - \hat{\mathbf{n}} \times \mathbf{H}^-(\mathbf{r})] \\ &- \hat{R}_c \hat{\mathbf{n}} \times \hat{\mathbf{n}} \\ &\times [\hat{\mathbf{n}} \times \mathbf{E}^+(\mathbf{r}) - \hat{\mathbf{n}} \times \mathbf{E}^-(\mathbf{r})],\end{aligned} \tag{1a}$$

$$\begin{aligned}\hat{\mathbf{n}} \times [\mathbf{H}^+(\mathbf{r}) + \mathbf{H}^-(\mathbf{r})] = \hat{R}_m \hat{\mathbf{n}} &\times [\hat{\mathbf{n}} \times \mathbf{E}^+(\mathbf{r}) - \hat{\mathbf{n}} \times \mathbf{E}^-(\mathbf{r})] \\ &+ \hat{R}_c \hat{\mathbf{n}} \times \hat{\mathbf{n}} \\ &\times [\hat{\mathbf{n}} \times \mathbf{H}^+(\mathbf{r}) - \hat{\mathbf{n}} \times \mathbf{H}^-(\mathbf{r})].\end{aligned} \tag{1b}$$

Here $\mathbf{E}^{\pm}(\mathbf{r})$ and $\mathbf{H}^{\pm}(\mathbf{r})$ represent the fields on the upper and the lower surfaces of the sheet, respectively; $\hat{R}_e$ and $\hat{R}_m$ are the scalar resistivity and conductivity describing the sheet, respectively; and $\hat{R}_c$ is a cross-coupling term. We remark that when $\hat{R}_c = 0$, the above conditions reduce to the resistive and conductive sheet or impedance surface defined by *Senior and Volakis* [1995] (see Table A1). The contribution of this paper is the introduction of the

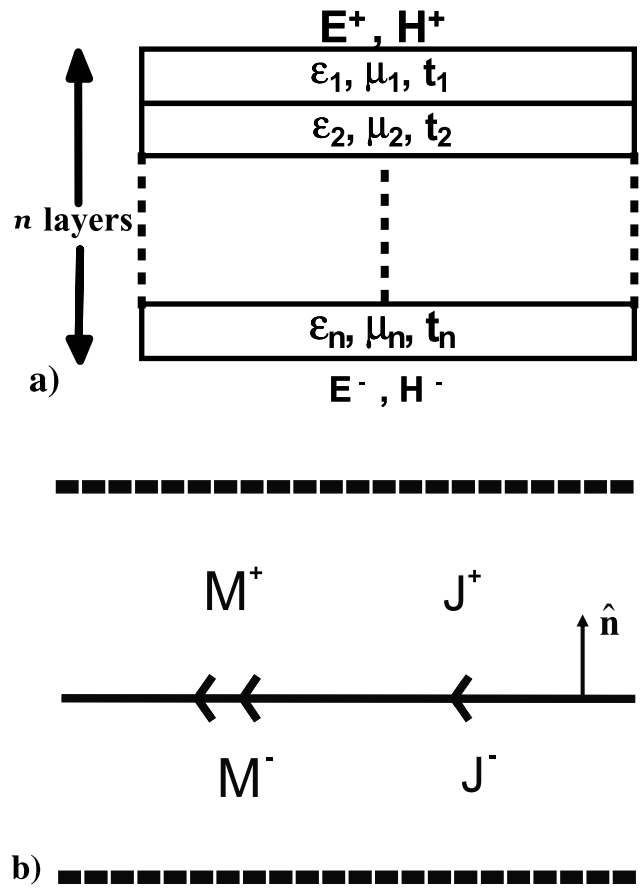

Figure 1. Geometry of the problem: (a) original problem and (b) equivalent problem.

coupling term $\hat{R}_c$ so that a more precise representation of the layered medium is possible. Rewriting equations (1a) and (1b) in matrix form, we have

$$\begin{bmatrix} \hat{\mathbf{n}} \times \mathbf{E}^-(\mathbf{r}) \\ \eta\hat{\mathbf{n}} \times \hat{\mathbf{n}} \times \mathbf{H}^-(\mathbf{r}) \end{bmatrix} = \begin{bmatrix} \Lambda_{11} & \Lambda_{12} \\ \Lambda_{21} & \Lambda_{22} \end{bmatrix} \begin{bmatrix} \hat{\mathbf{n}} \times \mathbf{E}^+(\mathbf{r}) \\ \eta\hat{\mathbf{n}} \times \hat{\mathbf{n}} \times \mathbf{H}^+(\mathbf{r}) \end{bmatrix}, \tag{2}$$

where $\Lambda_{ij}(i, j = 1, 2)$ are given by

$$\begin{aligned} \Lambda_{11} &= [1 + (1/2 - R_c)^2/R_eR_m] \\ &\quad /\{1 - [(1/4 - R_c^2)/R_eR_m]\}, \\ \Lambda_{12} &= -1/(R_m\{1 - [(1/4 - R_c^2)/R_eR_m]\}), \\ \Lambda_{21} &= -1/(R_e\{1 - [(1/4 - R_c^2)/R_eR_m]\}), \\ \Lambda_{22} &= \left[1 + (1/2 + R_c)^2/R_eR_m\right] \\ &\quad /\{1 - [(1/4 - R_c^2)/R_eR_m]\}, \end{aligned} \tag{3}$$

in which R_n ($\hat{R}_e = 2\eta\hat{R}_e$, $\hat{R}_m = -(2/\eta)R_m$, $\hat{R}_c = 2R_c$) with ($n = e, m, c$) represent the normalized quantities. To evaluate R_n, we proceed to match the reflection coefficients of the TBC sheet to that of the multilayered surface. For the TBC sheet we have that

$$\Gamma^{\pm}(\theta) = (2R_e\cos\theta - 2R_m/\cos\theta \pm 4R_c) / [4(R_eR_m + R_c^2) + 1 + 2R_e\cos\theta + 2R_m/\cos\theta], \tag{4a}$$

$$T(\theta) = [4(R_c^2 + R_eR_m) - 1] / [4(R_eR_m + R_c^2) + 1 + 2R_e\cos\theta + 2R_m/\cos\theta], \tag{4b}$$

where θ stands for the incidence angle, $T(\theta)$ refers to the transmission coefficient, and $\Gamma^{\pm}(\theta)$ are the reflection coefficients for the upper and lower faces of the layered sheet. Solving for R_n ($n = e, m, c$) gives

$$R_e = \{T^2(0) - [1 + \Gamma^+(0)][1 + \Gamma^-(0)]\} / \{\Gamma^+(0)\Gamma^-(0) - [1 - T^2(0)]^2\}/2, \tag{5a}$$

$$R_m = \left\{T^2(0) - \left[1 - \Gamma^+(0)\right]\left[1 - \Gamma^-(0)\right]\right\} \Big/ \left\{\Gamma^+(0)\Gamma^-(0) - \left[1 - T^2(0)\right]^2\right\}/2, \quad (5b)$$

$$R_c = \left[\Gamma^-(0) - \Gamma^+(0)\right] \Big/ \left\{\Gamma^+(0)\Gamma^-(0) - \left[1 - T^2(0)\right]^2\right\}/2. \quad (5c)$$

The above expressions can be used to compute R_n ($n = e$, m, c) from a knowledge of the reflection/transmission coefficients for some layered or inhomogeneous complex structure. These coefficients could be available from numerical analysis or measurements. Next, we use the conditions (2) to develop integral equations for scattering by structures involving TBC surfaces.

3. Surface Integral Equation

[5] To construct a surface integral equation, let us refer to Figure 2. The field interior and exterior to the closed boundary layer ∂B can be expressed by using the standard Stratton-Chu representations, namely,

$$\mathbf{E}_1(\mathbf{r}) = \theta_1(\mathbf{r})\{\mathbf{E}_i(\mathbf{r}) - \mathbf{\Theta}_1[\mathbf{J}_1, \mathbf{r}] + \mathbf{\Omega}_1[\mathbf{M}_1, \mathbf{r}]\} \quad \mathbf{r} \in B_1 \cup \partial B, \quad (6a)$$

$$\mathbf{H}_1(\mathbf{r}) = \theta_1(\mathbf{r})\left\{\mathbf{H}_i(\mathbf{r}) - \mathbf{\Omega}_1[\mathbf{J}_1, \mathbf{r}] - \frac{1}{(\eta_1)^2}\mathbf{\Theta}_1[\mathbf{M}_1, \mathbf{r}]\right\} \quad \mathbf{r} \in B_1 \cup \partial B, \quad (6b)$$

$$\mathbf{E}_2(\mathbf{r}) = \theta_2(\mathbf{r})\{-\mathbf{\Theta}_2[\mathbf{J}_2, \mathbf{r}] + \mathbf{\Omega}_2[\mathbf{M}_2, \mathbf{r}]\} \quad \mathbf{r} \in B_2 \cup \partial B, \quad (6c)$$

$$\mathbf{H}_2(\mathbf{r}) = \theta_2(\mathbf{r})\left\{-\mathbf{\Omega}_2[\mathbf{J}_2, \mathbf{r}] - \frac{1}{(\eta_2)^2}\mathbf{\Theta}_2[\mathbf{M}_2, \mathbf{r}]\right\} \quad \mathbf{r} \in B_2 \cup \partial B, \quad (6d)$$

with

$$\theta_n(\mathbf{r}) = \begin{cases} 1 & \mathbf{r} \in B_n, \\ 2 & \mathbf{r} \in \partial B, \\ 0 & \text{otherwise}, \end{cases} \quad (6e)$$

$$\mathbf{\Theta}_n[\mathbf{B}, \mathbf{r}] = \int_S \left\{j\omega\mu_n \mathbf{B}(\mathbf{r}') + \frac{j}{\omega\varepsilon_n}[\nabla' \cdot \mathbf{B}(\mathbf{r}')]\nabla\right\} \cdot G_n(\mathbf{r} - \mathbf{r}')ds', \quad (6f)$$

$$\mathbf{\Omega}_n[\mathbf{B}, \mathbf{r}] = \int_S \mathbf{B}(\mathbf{r}') \times \nabla G_n(\mathbf{r} - \mathbf{r}')ds'. \quad (6g)$$

In equations (6a)–(6d), $\mathbf{J}_k$ and $\mathbf{M}_k$ ($k = 1, 2$) are related to the tangential field components on the surface (see Figure 2),

$$\hat{\mathbf{n}} \times \mathbf{E}_1 = -\mathbf{M}_1 \quad ; \quad \hat{\mathbf{n}} \times \mathbf{H}_1 = \mathbf{J}_1, \quad (7a)$$

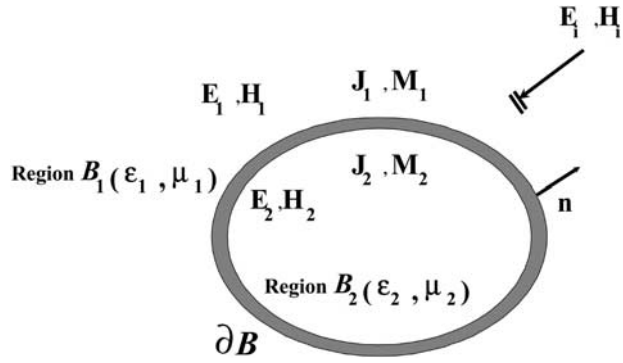

Figure 2. Surface for the application of the tensor boundary conditions.

$$\hat{\mathbf{n}} \times \mathbf{E}_2 = \mathbf{M}_2 \quad ; \quad \hat{\mathbf{n}} \times \mathbf{H}_2 = -\mathbf{J}_2, \quad (7b)$$

with the identification $\mathbf{E}_1 = \mathbf{E}^+$, $\mathbf{E}_2 = \mathbf{E}^-$, $\mathbf{H}_1 = \mathbf{H}^+$, and $\mathbf{H}_2 = \mathbf{H}^-$. On substituting equations (6a)–(6d) into the TBC conditions (2) and applying Galerkin's method, we obtain the matrix system

$$\begin{bmatrix} \Theta_1 - \frac{\eta\Lambda_{22}}{2\Lambda_{21}} & -\Omega_1 & -\frac{\eta}{2\Lambda_{21}} & 0 \\ \Omega_1 & \frac{1}{\eta_1^2}\Theta_1 - \frac{\Lambda_{11}}{2\eta\Lambda_{12}} & 0 & -\frac{1}{2\eta\Lambda_{12}} \\ \frac{\eta}{2}\left(\Lambda_{12} - \frac{\Lambda_{11}\Lambda_{22}}{\Lambda_{21}}\right) & 0 & \Theta_2 - \frac{\eta\Lambda_{11}}{2\Lambda_{21}} & -\Omega_2 \\ 0 & \frac{1}{2\eta}\left(\Lambda_{21} - \frac{\Lambda_{11}\Lambda_{22}}{\Lambda_{12}}\right) & \Omega_2 & \frac{1}{\eta_2^2}\Theta_2 - \frac{\Lambda_{22}}{2\eta\Lambda_{12}} \end{bmatrix} \cdot \begin{bmatrix} \mathbf{J_1} \\ \mathbf{M_1} \\ \mathbf{J_2} \\ \mathbf{M_2} \end{bmatrix} = \begin{bmatrix} \mathbf{E^i} \\ \mathbf{H^i} \\ 0 \\ 0 \end{bmatrix}, \quad (8)$$

which can be solved for the unknown equivalent current densities $\mathbf{J}_k$ and $\mathbf{M}_k$ ($k = 1, 2$). In the case where $\varepsilon_1 = \varepsilon_2$; $\mu_1 = \mu_2$ and $R_c = 0$, equation (8) reduces to the matrix equation

$$\begin{bmatrix} \Theta_1 - \frac{\eta}{2}\frac{\Lambda_{11}+1}{\Lambda_{21}} & -\Omega_1 \\ \Omega_1 & \frac{1}{\eta_1^2}\Theta_1 - \frac{1}{2\eta}\frac{\Lambda_{22}+1}{\Lambda_{12}} \end{bmatrix} \begin{bmatrix} \mathbf{J} \\ \mathbf{M} \end{bmatrix} = \begin{bmatrix} \mathbf{E^i} \\ \mathbf{H^i} \end{bmatrix}, \quad (9)$$

in which we set $\mathbf{J} = \mathbf{J}_1 + \mathbf{J}_2$ and $\mathbf{M} = \mathbf{M}_1 + \mathbf{M}_2$.

4. Numerical Results

[6] To demonstrate the application of the TBCs we consider two examples. For the first example we consider an air-filled dielectric shell. The shell's thickness is $\lambda_0/50$ with $\varepsilon_r = 1.75 - j0.3$ and $\mu_r = 1$ with the inner/outer radius of the sphere being $0.18\lambda_0/0.2\lambda_0$. For this example, about 1440 surface unknowns were used to explicitly model the sphere using the traditional moment method (MOM) approach. In contrast, the

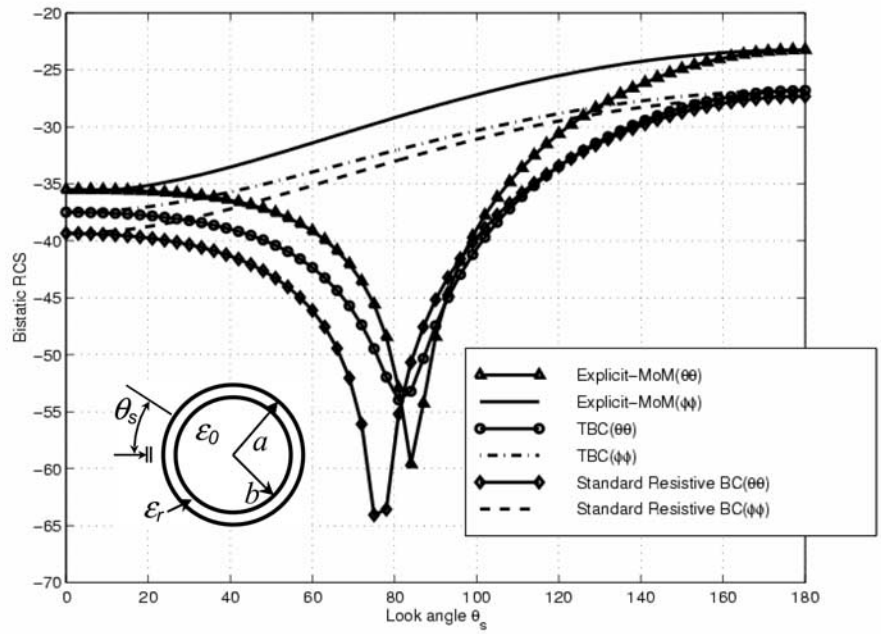

Figure 3. Bistatic RCS for a dielectric shell as computed by (1) rigorous integral equation approach, (2) TBC model, and (3) traditional resistive sheet model.

single TBC surface required 720 unknowns, and as seen in Figure 3 the radar cross section (RCS) results are in good agreement with the reference data denoted as ''explicit MOM'' in the figure. Except at pattern nulls we can generally state that the difference between TBC curves and the reference data is less than 2 dB. Given the small radius of the sphere, such an agreement is surprisingly remarkable and is likely attributed to poor modeling of the interactions within the interior boundaries. For this example, the specific resistivity parameters are

$$R_e = -4.2404 + j8.9811, \quad R_m = 141.1000 + j62.4430, \quad R_c = 0. \tag{10}$$

Using these in equations (3) we obtain the TBC matrix as follows:

$$\mathbf{\Lambda} = \begin{bmatrix} 0.9998 - j0.0002 & -0.0059 + 0.0026 \\ 0.0430 + j0.0910 & 0.9998 - j0.0002 \end{bmatrix}. \tag{11}$$

To better address the significance of the proposed TBC, Figure 3 also includes RCS curves computed using the standard resistive boundary condition instead of the TBC. The corresponding surface resistivity used in the resistive sheet condition was $R_s = 3.6587 - j9.1468$ [*Senior and Volakis*, 1995]. As seen, the TBC model provides substantially more accurate results whereas the simpler resistive sheet model is >5 dB in error.

[7] As a second example, we consider a dielectric sphere ($\varepsilon_{r2} = 4 + j0.0$, $\mu_r = 1 + j0$) which is coated by the same dielectric shell as before ($\varepsilon_r = 1.75 - j0.3$, $\mu_r = 1 + j0$). For this particular case, we again impose the TBC on the inner boundary of the sphere. For reference purposes, the explicit values of the resistivity parameters are as follows:

$$R_e = 1.0551 + j0.0922, \quad R_m = 3.7178 - j0.1638, \quad R_c = -1.5206 - j0.1094, \tag{12}$$

resulting in the TBC matrix

$$\mathbf{\Lambda} = \begin{bmatrix} 1.3366 - j0.0100 & -0.1763 - j0.0006 \\ -0.6143 + j0.0789 & 0.8292 - j0.0039 \end{bmatrix}. \tag{13}$$

Note that the presence of the inner dielectric sphere causes a nonzero R_c constant, and as a result this particular TBC is expected to have a substantially

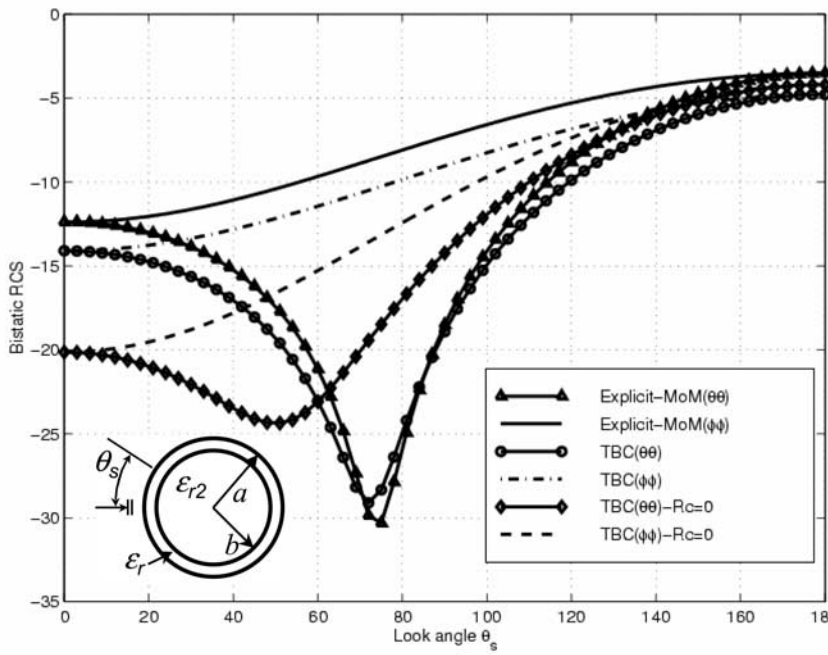

Figure 4. Bistatic RCS for a dielectric sphere coated by a dielectric shell as computed by (1) rigorous integral equation approach, (2) TBC model, and (3) TBC model with $R_c = 0$.

different character than the traditional resistive sheet. The corresponding RCS curves given in Figure 4 demonstrate that the TBC model is quite accurate. Better agreement with standard MOM is of course expected as the surface radius or the dielectric constant of the inner sphere is increased. A more clear impression of the new TBC model for layered structures is obtained when we arbitrarily set $R_c = 0$ (see Figure 4). The corresponding RCS curves are now substantially in error (more than 7 dB in the 0°–40° and 70°–100° sector), indicating the importance of the cross-coupling terms between the resistive and conductive/magnetic sheets.

Table A1. Boundary Conditions and Resistivities for Different Materials[a]

Material	Boundary Condition	Resistivity, Conductivity, and Cross-Coupling Parameters
PEC	$\hat{\mathbf{n}} \times \mathbf{E}^+ = 0,\ \hat{\mathbf{n}} \times \mathbf{E}^- = 0$	$R_e = 0,\ R_m = \infty,\ R_c = 0$
Resistive	$\hat{\mathbf{n}} \times [\mathbf{E}^+ + \mathbf{E}^-] = R\hat{\mathbf{n}} \times \hat{\mathbf{n}} \times [\mathbf{H}^+ - \mathbf{H}^-],$ $\hat{\mathbf{n}} \times [\mathbf{E}^+ - \mathbf{E}^-] = 0$	$R_e = R/\eta_0,\ R_m = \infty,\ R_c = 0$
Dielectric	$\hat{\mathbf{n}} \times [\mathbf{E}^+ - \mathbf{E}^-] = 0,$ $\hat{\mathbf{n}} \times [\mathbf{H}^+ - \mathbf{H}^-] = 0$	$R_e = \infty,\ R_m = 0,\ R_c = 0$
Impedance	$\hat{\mathbf{n}} \times \mathbf{E}^+ = Z^+ \hat{\mathbf{n}} \times \hat{\mathbf{n}} \times \mathbf{H}^+,$ $\hat{\mathbf{n}} \times \mathbf{E}^- = -Z^- \hat{\mathbf{n}} \times \hat{\mathbf{n}} \times \mathbf{H}^-$	$R_e = \dfrac{Z^+Z^-}{Z^+ + Z^-}, R_m = \dfrac{1}{Z^+ + Z^-},$ $R_c = \dfrac{Z^- - Z^-}{2(Z^+ + Z^-)}$

[a] PEC, perfect electric conductor.

5. Conclusion

[8] In this paper, we proposed a new class of tensor boundary conditions for modeling multilayered thin structures. The new boundary conditions were developed from knowledge of the reflection and transmission coefficients. Because the new tensor boundary conditions involve more degrees of freedom as compared to simpler conditions, they provide much more accurate simulation of complex material layers without a need to use computationally intensive volume formulation. Two numerical examples were included for preliminary validation of the proposed boundary conditions.

Appendix A

[9] For special values of the resistivity parameters the TBCs can be reduced to the simple first-order boundary conditions. Table A1 shows the boundary conditions and the resistivity parameters for different types of materials. Elements of the Λ matrices can easily be found by introducing the listed resistivity, conductivity, and cross-coupling parameters into equation (3).

References

Harrington, R. F., and J. R. Mautz, An impedance sheet approximation for thin dielectric shells, *IEEE Trans. Antennas Propag.*, *AP-36*, 531–534, 1975.

Mitzner, K. M., Effective boundary conditions for reflection and transmission by an absorbing shell of arbitrary shape, *IEEE Trans. Antennas Propag.*, *AP-16*, 706–712, 1968.

Puska, P. P., S. A. Tretyakov, and A. H. Sihvola, Approximate impedance boundary conditions for isotropic multilayered media, *IEE Proc., Part H: Microwaves Antennas Propag.*, *146*(2), 163–166, 1999.

Ricoy, M. A., and J. L. Volakis, Derivation of generalized transition/boundary conditions for planar multiple-layer structures, *Radio Sci.*, *25*(4), 391–405, 1990.

Senior, T. B. A., and J. L. Volakis, *Approximate Boundary Conditions in Electromagnetics*, Inst. of Electr. Eng., London, 1995.

D. C. Ross, Sikorsky Aircraft Corporation, 6900 Main Street, Stratford, CT 06497-9129, USA.

E. Topsakal and J. L. Volakis, Radiation Laboratory, Department of Electrical Engineering and Computer Science, University of Michigan, 3328 EECS Building, 1301 Beal Avenue, Ann Arbor, MI 48109-2122, USA. (topsakal@eecs.umich.edu; volakis@eecs.umich.edu)